International Microbiology
https://doi.org/10.1007/s10123-026-00882-5

RESEARCH

Antimicrobial, antibiofilm, and molecular docking evaluation of silver nanoparticles biosynthesized from *Ocimum campechianum* against *Staphylococcus* spp

Natilene Silva dos Santos[1] · Nayara Andreo[1] · Arun Kumar Jaiswal[1] · Milena Lima Guimarães[2] · Tania Maria Sarmento da Silva[3] · Helinando Pequeno de Oliveira[2] · Mateus Matiuzzi da Costa[1]

Received: 18 May 2026 / Revised: 30 July 2026 / Accepted: 5 August 2026

Abstract

Antimicrobial resistance and the overuse of antimicrobials have driven the search for innovative therapies, particularly those based on natural compounds and medicinal plant derivatives, aiming to develop new drugs. This study aimed to investigate the antimicrobial and antibiofilm activities of crude ethanolic extract of *O. campechianum* (CEE-OC), and commercial (AgNPs-C), non-commercial (AgNPs-NC), and *Ocimum campechianum*-biosynthesized (AgNPs-OC) silver nanoparticles, against 21 *Staphylococcus* spp. isolates. Antimicrobial activity of rosmarinic acid (RA) against six isolates was also determined. The minimum inhibitory concentration (MIC) of CEE-OC ranged from 6,250 to 781.25 µg/mL, showing the highest antimicrobial activity among the substances evaluated. AgNPs-OC exhibited MIC values approximately fourfold lower than those of CEE-OC. In contrast, AgNPs-C and AgNPs-NC showed no antimicrobial activity at the concentrations tested. CEE-OC and AgNPs-OC inhibited biofilm formation but had no effect on established biofilms. Molecular docking analysis suggested a potential interaction between RA and the NorA efflux pump protein. The results indicated that *O. Campechianum* extract and biosynthesized silver nanoparticles may represent promising antimicrobial alternatives, although further studies are needed to elucidate the mechanisms underlying their activity.

Keywords Antimicrobial alternatives · Basil · Biofilm inhibition · Green synthesis · Molecular docking · Nanotechnology

✉ Mateus Matiuzzi da Costa
mmatiuzzicosta@gmail.com

Natilene Silva dos Santos
natilene.vet@gmail.com

Nayara Andreo
nayarandreo@gmail.com

Arun Kumar Jaiswal
arunjaiswal1411@gmail.com

Milena Lima Guimarães
milenalimaguimaraes@gmail.com

Tania Maria Sarmento da Silva
sarmentosilva@gmail.com

Helinando Pequeno de Oliveira
helinando@gmail.com

[1] Laboratory of Animal Microbiology, Federal University of the São Francisco Valley (UNIVASF), Campus of Agricultural Sciences, Petrolina, Pernambuco 56300-000, Brazil

[2] Laboratory of Impedance Spectroscopy of Organic Materials, Institute of Material Sciences, Federal University of the São Francisco Valley (UNIVASF), Juazeiro, Bahia 48902-300, Brazil

[3] Laboratory of Chemistry, Federal Rural University of Pernambuco, Recife 52171-900, Brazil

Published online: 08 August 2026

Introduction

The ability of *Staphylococcus* spp. to form biofilms favors their survival in different environments, facilitating the persistence and dissemination of resistant strains (Santos et al. 2025; Rather et al. 2021). Although conventional antibiotics remain the main strategy for bacterial infection management, the increasing emergence of multidrug-resistant strains has highlighted the urgent need for alternative antimicrobial approaches (Jiang et al. 2023).

Natural products and green nanotechnology have emerged as promising strategies due to their structural diversity and mechanisms of action distinct from conventional antimicrobials. Among these strategies, plant-mediated synthesis of silver nanoparticles (AgNPs) has gained attention because it combines the antimicrobial properties of silver with the chemical diversity of plant metabolites, generating nanostructures with potential antibacterial and antibiofilm activity (Chinnasamy et al. 2024; Jiang et al. 2023; Calvo-Irabien 2025).

Several plant species, including *Ocimum tenuiflorum*, *Ocimum gratissimum*, *Pergularia tomentosa*, and *Malva parviflora*, have been explored as biological sources for AgNP synthesis, resulting in nanoparticles with enhanced biological activities and potential applications against resistant microorganisms (Varghese et al. 2024; Aldayel 2024; Al-Audah et al. 2025).

The green synthesis approach is also considered advantageous due to its sustainable characteristics and reduced environmental impact compared with conventional chemical synthesis methods (Shah et al. 2025).

Among medicinal plants, *Ocimum campechianum* (Lamiaceae) has been investigated due to its bioactive compounds, such as rosmarinic acid (RA) and eugenol, which are associated with antimicrobial and pharmacological properties (Tacchinni et al. 2020; Scalvenzi et al. 2019; Ruiz-Vargas et al., 2019). These bioactive molecules may contribute to the synthesis of plant-mediated AgNPs. However, despite its phytochemical potential, the application of *O. campechianum* as a biological source for silver nanoparticle synthesis and its possible role in antimicrobial mechanisms remains poorly explored.

Although previous studies have investigated the antimicrobial properties of *Ocimum* species and silver nanoparticles, comparative evaluations of commercial, chemically synthesized, and *O. campechianum*-mediated AgNPs against *Staphylococcus* spp. isolates remain limited. Additionally, molecular docking analysis may provide insights into the interactions of plant-derived compounds with the NorA efflux pump and their potential contribution to antimicrobial activity.

We hypothesized that *O. campechianum*-mediated AgNPs would exhibit enhanced antimicrobial and antibiofilm activity due to synergistic interactions between silver nanoparticles and plant-derived metabolites. Therefore, this study aimed to evaluate the antimicrobial and antibiofilm activities of commercial (AgNPs-C), chemically synthesized (AgNPs-NC), and *O. campechianum*-biosynthesized (AgNPs-OC) silver nanoparticles, as well as the crude ethanolic extract of *O. campechianum* (CEE-OC) and rosmarinic acid (RA), against *Staphylococcus* spp. isolates. Additionally, molecular docking analysis was performed to investigate potential interactions between plant-derived compounds and the NorA efflux pump.

Materials and methods

Ethics committee approval

The research was approved by both CEUA (Comitê de Ética em Uso de Animais — Animal Use Ethics Committee) of the Federal University of the São Francisco Valley (UNIVASF), registered under No. 0002/300,823, and CEP (Comitê de Ética em Pesquisa — Research Ethics Committee), registered under No. 6.013353. The isolates were identified under registration number AEEA0F9 and deposited in the Sistema Nacional de Gestão do Patrimônio Genético (National Genetic Heritage Management System). Furthermore, all human-derived bacterial isolates were anonymized and de-identified, with no access to any patient information; therefore, informed consent was not required.

Extraction and characterization of the crude ethanolic plant extract of *O. campechianum*

Wild sweet basil (*Ocimum Campechianum* - OC) was collected in the municipalities of São Gabriel, Irecê, and Cotegipe, all located in the state of Bahia. The plant was identified and registered under the number AB7B2FE, and deposited in the Sistema Nacional de Gestão do Patrimônio Genético (National Genetic Heritage Management System). Crude ethanol extract (CEE-OC) was produced from the whole plant (leaves, seeds, and stem) in the Laboratory of Bromatology and Animal Nutrition of the Federal University of the São Francisco Valley, UNIVASF-CCA, and the extraction was carried out according to the methodology of (Da Silva et al. 2016).

An extract sample was subjected to phytochemical characterization using Ultra-Performance Liquid Chromatography (UPLC) at the Laboratory of Phytochemical Bioprospecting, Department of Chemistry, Federal Rural University of Pernambuco (UFRPE). For UPLC analysis, five grams of the plant extract was used and subsequently dissolved in one milliliter (mL) of an acetonitrile: water solution with 0.1% formic acid (1:1, v/v). The solution was filtered

through a 0.2 µm membrane filter and injected into the ultra-performance liquid chromatography system coupled with a diode array detector and quadrupole time-of-flight mass spectrometry analysis (UPLC-DAD-qTOF-MS/MS). The analysis was obtained using the XEVO-G2XSQTOF mass spectrophotometer (Waters, Manchester, UK), which was connected to an ACQUITY UPLC System (Waters, Milford, MA, USA). Data were obtained through UPLC-DAD-qTOF-MS/MS according to the conditions described by (Souza et al. 2018). The compounds rutin and rosmarinic acid were compared with their respective standards.

Synthesis of silver nanoparticles

Commercial nanoparticles (AgNPs-C) were obtained from Sigma-Aldrich® at a concentration of 20 µg/mL and a size equivalent to 20 nm. Non-commercial silver nanoparticles (AgNPs-NC), or synthesized chemically, were obtained according to the methodology described by Freire et al. (2018), with modifications. The process was based on the reduction of silver nitrate ($AgNO_3$) and trisodium citrate and carried out at the Laboratory of Impedance Spectroscopy of Organic Materials (LEIMO) at UNIVASF, Campus Juazeiro. The biosynthesis (green synthesis/biogenic synthesis) of silver nanoparticles using the *O. campechianum* extract was also performed at LEIMO, according to the methodology described by Guimarães et al. (2020), with adaptations. A green synthesis route was used, with the crude ethanolic extract of wild sweet basil as a bioreductive agent.

The silver nanoparticles were then prepared in a neutral medium (pH 7) for synthesis using the *O. campechianum* extract (CEE-OC), with the pH adjusted by the addition of sodium hydroxide (NaOH, 0.1 M) and hydrochloric acid (HCl, 0.1 M) in aqueous solution. The reduction reaction of silver ions occurred between 98 and 100 °C, and the reaction kinetics were monitored at fixed time intervals (15, 30, 45, and 60 min) using ultraviolet-visible spectroscopy (UV-Vis). For this analysis, 3 mL aliquots were measured by UV-Vis spectroscopy over a wavelength range of 400–800 nm using a UV-Vis spectrophotometer (Hach DR5000) with a resolution of 1 nm to monitor nanoparticle formation. Nanoparticle formation was confirmed considering the SPR (Surface Plasmon Resonance) band characteristic of AgNPs. Data were collected and subsequently plotted.

To evaluate the particle size distribution, dynamic light scattering (DLS) measurements were performed using a Malvern Zetasizer Nano particle analyzer. Measurements of the polydispersity index (PDI) and hydrodynamic diameter of the suspended particles were obtained. The data obtained were analyzed using the equipment software (ZetaSizer v3.30, Malvern). The morphological characterization of the samples was performed by scanning electron microscopy (SEM), using a Vega 3XM scanning electron microscope (Tescan), operating at an acceleration voltage of 20 kV. The images obtained were used for qualitative analysis of the morphology, size, and dispersion of the nanoparticles using Image J® software. To provide a more comprehensive understanding of the interaction between the biomolecules present in CEE-OC and the AgNPs-OC, Fourier transform infrared spectroscopy (FTIR) was employed. The analyses were conducted over the spectral range of 4000 to 500 cm^{-1}, allowing the identification of characteristic functional groups and possible structural modifications resulting from interaction between the components.

Bacterial samples

Twenty isolates of the genus *Staphylococcus* sp. from different species were used in this study (Table 1), with five isolates from each source: food (cheese and meat products); bovine mastitis; canine otitis; and human infections. All isolates were identified and standardized at the Laboratory of Animal Microbiology and Immunology of UNIVASF - Campus of Agricultural Sciences (CCA), except for four *S. aureus* bovine mastitis isolates obtained from the bacterial collection of the same laboratory and five human infection isolates, which were provided and identified by the University Hospital (HU) at UNIVASF. The American Type Culture Collection (ATCC) strain of *S. aureus* (ATCC 25923) was used as a control.

Table 1 Identification and origin of the isolates analyzed in the study

Isolate identification	Genus or species	Source
C1; C2; Q1, Q2; Q3	*Staphylococcus* sp.	Food
73853	*Staphylococcus* sp.	Bovine mastitis
AL01; AL02; WE08; WE09	*S. aureus*	Bovine mastitis
TH; ZO; AR; 141/15; FIL	*Staphylococcus* sp.	Canine otitis
IMA	*S. cohnii*	Human infection
EOC	*S. epidermidis*	Human infection
JCS	*S. capitis*	Human infection
RPS	*S. haemolyticus*	Human infection
HUT	*S. aureus*	Human infection

Evaluation of antimicrobial activity

Antimicrobial susceptibility testing

The agar disk diffusion method was used as a susceptibility test, as recommended by the Clinical and Laboratory Standards Institute (CLSI 2018). Samples were cultured in Brain Heart Infusion (BHI) medium and incubated at 37 °C for 24 h in a bacteriological incubator. The bacterial suspension was then prepared and adjusted to 3×10^7 CFU/mL. Antibacterial activity was evaluated using disks containing clinically relevant antimicrobials: Linezolid 10 mcg, Azithromycin 10 mcg, Levofloxacin 5 mcg, Chloramphenicol 30 mcg, Tetracycline 30 mcg, Rifampicin 5 mcg, Clindamycin 2 mcg, Oxacillin 1 mcg, Gentamicin 10 mcg, Cefoxitin 30 mcg, Cefalotin 30 mcg, Penicillin G (10 IU), and Norfloxacin 10 mcg. The plates were incubated at 37 °C for 24 h, and the results were read by measuring the diameter of the inhibition zones. Multiresistant isolates were identified according to Schwarz et al. 2010; and the Multiple Antibiotic Resistance Index (MDR) was calculated as described by Krumperman (1983).

Microdilution in broth

The Minimum Inhibitory Concentration (MIC) and the Minimum Bactericidal Concentration (MBC) of the substances (CEE-OC, AgNPs-C, AgNPs-NC, and AgNPs-OC) were determined according to CLSI document M100 from the Clinical and Laboratory Standards Institute (CLSI, 2018) against 21 *Staphylococcus* spp. Isolates. The MIC and MBC of the isolated compound rosmarinic acid (RA), were also determined against five isolates, two of which were susceptible [*S. epidermidis* (EoC) and *S. capitis* (JCS)] and two resistant [*Staphylococcus* sp. (Q1) and *S. aureus* (HUT)], as well as ATCC 29,213 (*S. aureus*). Stock solutions of the substances (concentrations of 25,000 µg/mL – CEE-OC; 20 µg/mL – AgNPs-C; proportionally estimated – AgNPs-NC and AgNPs-OC; 10 mg/mL – rosmarinic acid) were serially diluted in 96-well plates (KASVI) with the final volume of 100 µL. The estimated proportions of AgNPs-NC and AgNPs-OC were based on final dilution ratios of 1:1, 1:2, 1:4, 1:8, 1:16, 1:32, 1:64, and 1:128 µg/mL, and the concentration of bacterial inocula was adjusted to 1.5×10^6 CFU/mL. The plates were incubated at 37 °C for 24 h. The contents of the wells were then inoculated onto plates containing Mueller-Hinton agar (MH agar) and incubated for an additional 24 h at 37 °C to determine the MBC. Then, 30 µL of 1% 2,3,5-Triphenyl-tetrazolium chloride (TTC) was added to each well, and the plate was incubated at 37 °C for approximately 1 h to determine the MIC. All assays were performed in technical and biological triplicates, including bacterial viability control and a diluent control.

Checkerboard

The synergistic potential of CEE-OC with the three substances (AgNPs-OC, AgNPs-C, and AgNPs-NC) was evaluated using the checkerboard assay according to the methodology of (Lee et al. 2012) againsts *Staphylococcus* spp isolates. The initial concentrations of CEE-OC and AgNPs-OC were 4x or 2x the MIC, depending on the isolate, while AgNPs-C and AgNPs-NC were used undiluted. The interaction between CEE-OC and AgNPs-OC was analyzed in all isolates, however, for the combinations of CEE-OC with AgNPs-C and CEE-OC with AgNPs-NC, two isolates considered susceptible (*S. capitis* and *S. epidermidis*) and one isolate with higher resistance (*Staphylococcus* sp. and *S. aureus*) were selected. The interpretation of the effects of each substance and their combinations was determined using the Fractional Inhibitory Concentration Index (FICI), classified as synergistic ($FICI \leq 0.5$), additive ($0.5 < FICI \leq 1$), indifferent ($1 < FICI \leq 2$), and antagonistic ($FICI > 2$).

Antibiofilm production and activity

Quantification of biofilm production

Quantification of biofilm production was performed by microplate adhesion assay. The bacterial inoculum was set at 3×10^7 CFU/mL in Trypticase Soy Broth (TSB) supplemented with 0.25% glucose (TSBg). The 96-well plate (KASVI) contained 195 µL of TSBg, followed by the addition of 5 µL of the adjusted bacterial suspension. The microplates were incubated in a bacteriological incubator at 37 °C for 24 h. After incubation, the microplates were washed three times with sterile distilled water and dried at room temperature for approximately 5 min (Merino et al. 2009). To fix the biofilm, 150 µL of methanol P.A. (ACS®) was added, and the plates were incubated for 20 min at room temperature. The contents were discarded, and the microplates were allowed to dry overnight by inversion on paper towels (Stepanovic et al. 2007). Next, the wells were stained with 100 µL of 0.25% gentian violet for 5 min. After staining, the wells were gently washed three additional times with 200 µL of distilled water. Finally, 200 µL of an alcohol-acetone solution (80:20 ratio) [absolute alcohol 99.8% P.A. (NEON, São Paulo, Brazil)] was added, and the absorbance was measured at 620 nm using an Expert Plus-UV microplate reader. TSBg without bacterial inoculation was used as a negative control and all assays were performed in technical and biological triplicates. Biofilm production was determined according to Stepanovic et al. (2000) as follow: No biofilm production ($ODs \leq ODc$); Weak biofilm production ($ODc < ODs \leq 2 \times ODc$); Moderate biofilm production ($2 \times ODc < ODs \leq 4 \times ODc$); Strong biofilm production (4

×ODc < ODa), where ODc is the optical density of the control and ODs is the optical density of the sample.

Biofilm interference

Interference of CEE-OC, AgNPs-C, AgNPs-NC, and AgNPs-OC with biofilm formation and established biofilm was determined. The interference protocol in biofilm formation was performed according to the methodologies of Merino et al. (2009) and Nostro et al. (2007), with modifications. The bacterial inoculum was set in TSBg (KASVI) to a concentration of 3×10^5 CFU/mL. Following this, 100 µL of the adjusted bacterial inoculum was added to a 96-well microplate (KASVI) along with 100 µL of each of the substances mentioned, resulting in final concentrations of ½ MIC for: CEE-OC, AgNPs-C, AgNPs-NC and AgNPs-OC; and ¼ MIC for CEE-OC and AgNPs-OC. After 24 h of incubation in a bacteriological incubator, the microplates were subjected to the same washing, fixation, resuspension, staining, and reading procedures described for biofilm quantification. Similarly, interference with established biofilm was assessed using the same procedures as those described for biofilm formation, based on the methodologies of Merino et al. (2009) and Stepanovic et al. (2007), with modifications.

The effect of the substances was determined by preparing the bacterial suspension in TSBg at 6×10^6 CFU/mL. Next, 195 µL of TSBg was added to each well of the microplate along with 5 µL of the adjusted bacterial inoculum. The plates were then incubated in a bacteriological incubator at 37 °C for 24 h. After incubation, the microplates were washed three times with sterile distilled water. To achieve final concentrations of 2x MIC, 1x MIC, and ½ MIC, the substances CEE-OC and AgNPs-OC were diluted with sterile distilled water, except for AgNPs-C and AgNPs-NC, which were used undiluted, as no MIC was reached at the tested concentrations. Afterwards, the optical density (OD) was measured at 620 nm at 0 (zero) and 24 h of incubation. The results for stablished biofilm interference were interpreted using the following equation: mean $OD_{(24h)}$ / mean $OD_{(0h)}$ ×100 (Adapted from Nostro et al. 2007), where: =100 indicates no change; >100 indicates an increase in biofilm; <100 indicates biofilm reduction. The assays were performed in technical and biological triplicates.

Statistical analysis

The biofilm interference results were analyzed using parametric multiple comparisons tests, specifically Two-way ANOVA with the posthoc test of Tukey. Statistical analyses were performed using GraphPad Prism 8 software, and results were plotted as mean ± standard deviation. For all tests, a p-value < 0.05 was considered statistically significant.

Molecular docking of rosmarinic acid

The 3D structure of the NorA protein was retrieved from the Data Bank database (RCSB, https://www.rcsb.org/structure/7LO7). Data structure was submitted to the MGLtool program and the AutoDock interface was used to prepare the receptor. Kollman charges were added to the receptor (NorA protein) along with the binding sites Phe16, Phe140, Phe303, Phe306, Asn137, Arg98, Glu222, Asp307, and Arg310, which were selected based on structural studies to guide the docking analysis (Brawley et al. 2022). The chemical structure of rosmarinic acid was obtained from the PubChem database (https://pubchem.ncbi.nlm.nih.gov/compound/5281792) and used as a ligand. For the analysis and calculation of binding energy, the molecular docking tool AutoDock Vina (Eberhardt et al. 2021) and the visualization software Chimera were used to identify potential hydrogen-bond interactions between the ligand and the NorA binding pocket.

Results and discussion

Ultra-Performance Liquid Chromatography (UPLC) revealed the predominant presence of phenolic compounds — including flavones, quercetin, and rosmarinic acid — in the ethanolic extract of *O. campechianum* (CEE-OC) (Table 2).

Table 2 Characterization of crude ethanolic extract of *O. campechianum* (CEE-OC) compounds through UPLC-DAD-qTOF-MS/MS analysis

Compounds	RT (min)	λmax (nm)	$[M+Na]^+$ (m/z)	$[M+H]^+$ (m/z)	MS/MS	Identification
1	2.64	255.353	633.1406	611.1606	303	Rutin*
2	2.70	255.352	487.0846	465.1027	303	Quercetin glucosides
3	3.38	329-	383.0616	361.0624	-	Rosmarinic Acid
4	5.35	288-	355.0747	333.0937	197	Trihydroxy-dimethoxy flavanone I
5	5.44	288-	355.0747	333.0937	197	Trihydroxy-dimethoxy flavanone II
6	6.39	287-	369.0944	347.1125	997	Dihydroxy-trimethoxy flavanone
7	6.48	274.340	367.0788	345.0968	330.312	6-hydroxy-trimethoxy-luteolin
8	7.67	275.340	381.0945	359.1125	298	5-demethyl sinensetin
9	8.37	251.340	411.1051	389.1230	-	5-demethyl nobiletin

* Compared to the standard sample

Most compounds identified in CEE-OC were similar with those previously reported by Ruiz-Vargas et al., (2019), indicating a comparable chemical profile among samples of *O. campechianum*. These similarities may be related to the presence of conserved bioactive constituents commonly reported in this species; however, variations in phytochemical composition may occur due to environmental conditions, geographical origin, and genetic factors.

Furthermore, the results revealed a prominent abundance of rosmarinic acid (RA), which stood out compared to the other compounds in the maxג 329 class (Table 2). Although RA is a common metabolite in the Lamiaceae family, not all species contain it among their chemical constituents, making it a potential distinguishing component contributing to antimicrobial activity (Kernou et al. 2023).

According to Abdel-Aty et al. (2023), phenolic acids are important components in green synthesis, as they are present in the plant extract used for nanoparticle production.

The formation of AgNPs was initially evidenced by the color change of the reaction solution, from light yellow to brown, characteristic of the reduction of Ag^{+} ions and the formation of silver nanoparticles. This observation was confirmed by UV-Vis spectroscopy, which revealed a Surface Plasmon Resonance (SPR) band centered at 422 nm, characteristic of AgNPs. Monitoring the reaction at different time intervals revealed a gradual increase in the intensity of the SPR band, reaching a maximum at 60 min (Fig. 1A), indicating the evolution of the nanoparticle formation kinetics. This behavior is similar to that described in the literature for green syntheses of AgNPs, in which an increase in SPR band intensity accompanies the progressive formation of nanoparticles until the reaction stabilizes (Guimarães et al. 2020; Mandal et al. 2024).

Dynamic Light Scattering (DLS) characterization revealed a hydrodynamic size distribution ranging from 50.75 to 458.7 nm, with an average hydrodynamic diameter of 147.9 nm, maximum intensity in the 164.2 nm range, and a distribution width at half-height of 161.79 nm (Fig. 1B). The presence of particles larger than the nanometer range may be associated with the formation of aggregates or agglomerates, a phenomenon frequently observed in biosynthesized systems due to interactions between nanoparticles and biomolecules in the plant extract (Siddiqi et al. 2018). The polydispersity index (PDI) of 0.297 indicates a moderately homogeneous size distribution, with the coexistence of different particle populations.

The evaluation of colloidal stability showed a zeta potential of −29.5 mV, indicating a negatively charged surface, which may be associated with the adsorption of phytochemical compounds, such as phenolics and flavonoids, onto the AgNPs. A similar value was reported by Ashokkumar et al. (2024) for AgNPs synthesized with Ocimum sanctum (−29.2 ± 1.04 mV), supporting the production of nanoparticles with relatively good colloidal stability. These metabolities, described by Abdel-Aty et al. (2023) as reducing and stabilizing agents in the green synthesis of metallic nanoparticles, contribute to the electrostatic repulsion between the particles, favoring the stability of the suspension and reducing the tendency for aggregation (Ashokkumar et al. 2024; Mandal et al. 2024).

SEM characterization revealed nanoparticles with distinct morphologies and Energy-Dispersive X-ray Spectroscopy (EDS) elemental analysis confirmed the characteristic silver signal, complementing the morphological and compositional characterization of the AgNPs (Fig. 2).

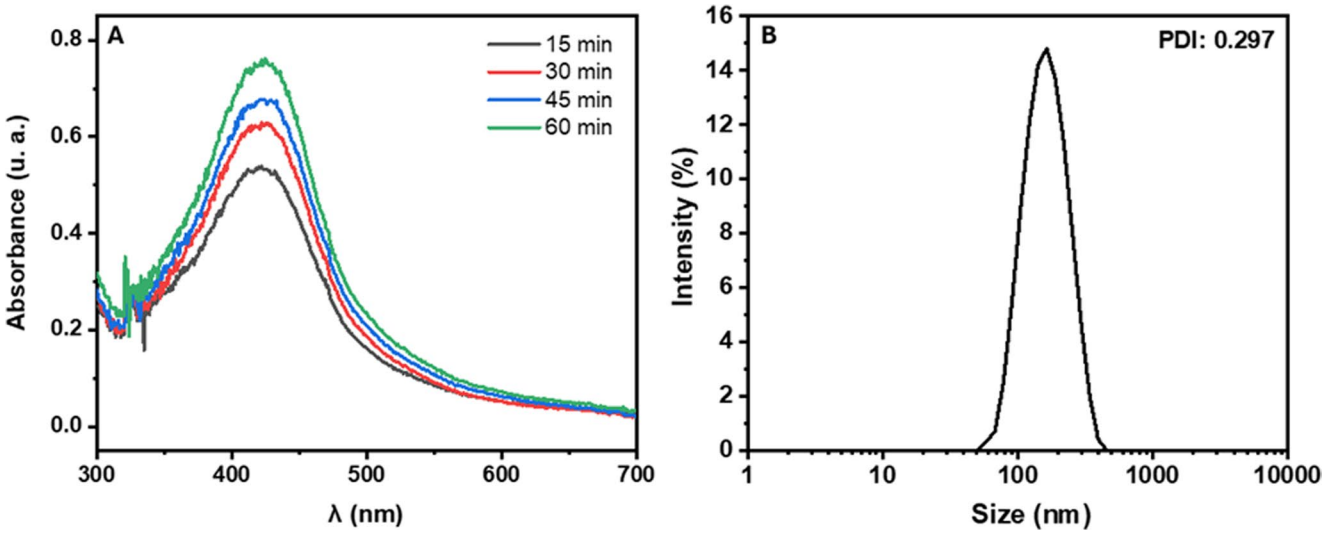

Fig. 1 (**A**) UV-Vis absorption spectrum; (**B**) Hydrodynamic size distribution and Polydispersity Index (PDI) obtained by Dynamic Light Scattering (DLS)

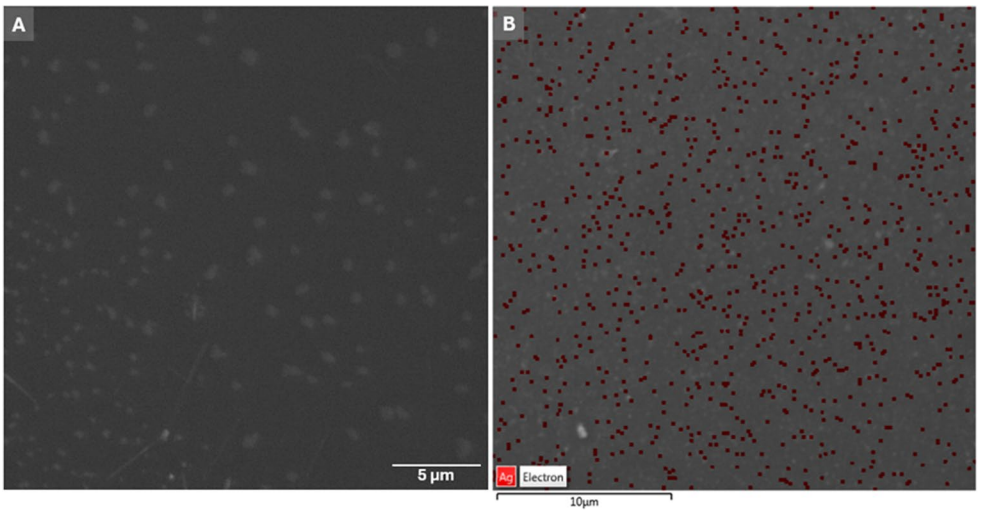

Fig. 2 (**A**) Scanning Electron Microscopy (SEM) image showing the morphology of the nanoparticles; (**B**) Energy-Dispersive X-ray Spectroscopy (EDS) spectrum superimposed on the SEM image

The FTIR spectra of the *O. campechianum* extract and the AgNPs showed characteristic bands of biomolecules frequently associated with the green synthesis of nanoparticles (Fig. 3). In the extract, the bands at 3433.43 cm^{-1} and 3447.90 cm^{-1} in the AgNPs-OC are attributed to the O–H stretching of hydroxyl groups present in alcohols and phenolic compounds. This attribution is consistent with the band at 3397.8 cm^{-1} described by Guimarães et al. (2020) and with the bands observed in AgNPs synthesized using species of genus *Ocimum*, such as *O. sanctum* (3406 cm^{-1}) *and O. basilicum (*3321.39 cm^{-1}), also related to the presence of hydroxyl groups from plant metabolites (Ashokkumar et al. 2024; Fatima et al. 2024). The bands at 2924.21–2854.77 cm^{-1} (extract) and 2929.03–2872.13 cm^{-1} (AgNPs) correspond to the C–H stretching of aliphatic groups in agreement with the bands described by Guimarães et al. (2020) (2949.3 cm^{-1}), Ashokkumar et al. (2024) (2939 and 2849 cm^{-1}) and by another study with *Ocimum* species, which reported bands at 2924.72 and 2853.53 cm^{-1} attributed to the same vibrations (Alex et al. 2024).

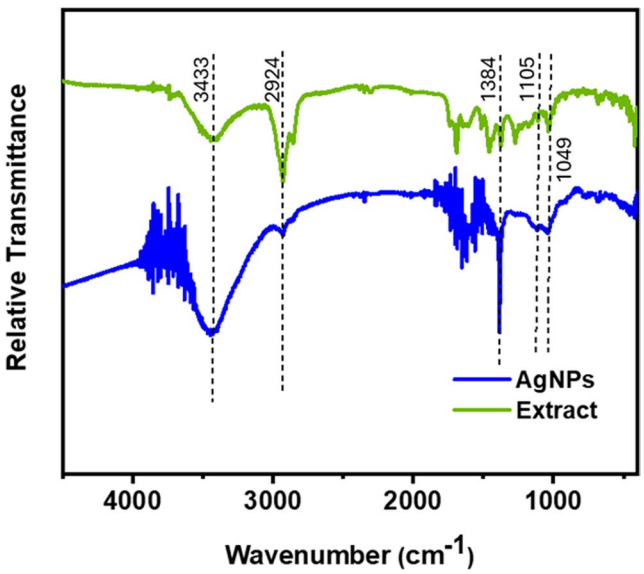

Fig. 3 Analysis by Fourier transform infrared spectroscopy (FTIR) of the *O. campechianum* extract (green curve) and biosynthesized AgNPs-OC (blue curve)

In the region of lower wavenumber, the AgNPs showed bands at 1384.94, 1105.3 e 1049.3 cm^{-1}. The band at 1384.94 cm^{-1} corresponds to the same spectral region described by Guimarães et al. (2020), who based on Halanwani (2017), attributed it to the presence of carboxylate/carboxylic groups. Similar bands were also observed in AgNPs synthesized from species of the genus *Ocimum* such as the bands at 1384.53 cm^{-1} described by Alex et al. (2024) and at 1396.65 cm^{-1} reported by Fatima et al. (2024). The bands at 1105.3 and 1049.3 cm^{-1} are compatible with vibrations involving C–O/C–C and C–OH groups, in agreement with Guimarães et al. (2020), and are also consistent with the band at 1105.71 cm^{-1} observed by Fatima et al. (2024) and with the bands between 1107.80 and 1124.83 cm^{-1} described by Alex et al. (2024). Together, these bands indicate that metabolites from the extract remained adsorbed onto the surface of the AgNPs after synthesis, acting as capping agents and contributing to the stabilization of the nanoparticles.

Regarding the susceptibility test, isolates from food and animal sources (mastitis and otitis) exhibited the highest resistance rates to the antimicrobials penicillin G (80.00% -12/15) and oxacillin (46.67% -7/15) from the penicillin class, followed by tetracycline (43.75% -7/15) and doxycycline (18.25% −3/15) from the tetracycline class. Additionally, 33.33% (5/15) of the isolates were resistant to gentamicin and rifampicin (aminoglycoside and macrolide classes, respectively), 26.67% (4/15) to norfloxacin, azithromycin, and chloramphenicol (fluoroquinolone, macrolide, and amphenicol classes, respectively), and 20.00% (3/15) to clindamycin and levofloxacin (lincosamide and quinolone

classes, respectively). No resistance was observed for linezolid (oxazolidinone class), cefalotin and cefoxitin (cephalosporin class). The high bacterial tolerance observed against the tetracycline and penicillin classes is likely attributable to the extensive use of antimicrobials from these classes in the treatment of *Staphylococcus* infections. This is particularly evident from the elevated resistance rates detected in isolates of food origin.

However, resistance is not only associated with these factors (Machado et al. 2020), but also with genetic factors and the ability of the bacteria to produce biofilm — a structure that provides protection, reducing antimicrobial penetration (Almatroudi et al. 2020). The high resistance rate of the isolates to the aminoglycoside class may be related to the presence of enzymes that modify the antimicrobial target (Bourbour et al. 2022; Wang et al. 2022; Khosravi et al. 2017; Szymanek- Majchrzak, et al., 2018). These findings are concerning, given the limited treatment options for severe cases and considering that this is the most used class of antimicrobials in hospitalized patients (Khosravi et al. 2017).

Similar resistance results were observed for the macrolide, amphenicol, and fluoroquinolone classes, which may be associated with genetic mutations that may contribute to bacterial survival (Kang et al. 2020; Manoharan et al. 2021; Huynh et al. 2023). However, the lack of resistance among the isolates to the cephalosporin and oxazolidinone classes may suggest the absence of resistance mechanisms associated with these antimicrobial classes.

Of the 15 isolates analyzed in this study, nine exhibited a Multiple Antibiotic Resistance Index (MDR) > 0.2. These included: four isolates from canine otitis — 141/15 (0.36), TH (0.27), AR (0.45), and ZO (0.45); three from food source — Q1 (0.45), Q3 (0.36), and C2 (0.36); and two from bovine mastitis — 73,853 and AL02, both with a MARI of 0.27. These same isolates were classified as multidrug-resistant (MDR). The values found in this study suggest that there is a relationship between the resistance characteristics of the different isolates and their various origins, such as food and animal sources, possibly indicating that the misuse of antimicrobials in food-producing animals may contribute to the dissemination of antimicrobial resistance among these different sources. Thus, the distribution of resistance and virulence genes is inferred based on the multiple drug resistance (MDR) profile of the isolates analyzed in this study. Regarding the five human-derived isolates (Table 3), laboratory reports revealed a 100% prevalence of resistance markers associated with beta-lactamase production and methicillin resistance.

The antimicrobials classes used (Table 3) differ from those employed in the Laboratory of Microbiology - UNIVASF, Campus of Agricultural Sciences (CCA) due to the high level of resistance typically expected in infections among hospitalized patients. However, similar to the resistance profile observed in animal- and food-derived isolates, the human-derived isolates also showed high resistance to antimicrobials from the penicillin and macrolide classes, with rates of 100% and 90%, respectively. In contrast, no resistance was observed to the oxazolidinone, lipopeptide and glycopeptide classes.

The resistance profile to the penicillin class observed among the isolates analyzed in this study may be related to horizontal transmission between hosts (Pugazhendhi et al. 2020). Therefore, it is plausible to suggest the existence of a cycle of transmission of bacterial resistance factors and the probable transmission of MRS from infected humans to pets. The suggested transmission cycle may be related to direct contact between these infected hosts, or even inadequate cleaning and processing practices, as well as the consumption of food contaminated after processing (Cotter et al. 2023).

The resistance markers identified in the human-derived isolates were assessed through phenotypic characterization using the BD Phoenix™ M50 automated identification system, which is based on inhibitory microdilutions of the antimicrobial oxacillin (1 mcg). The markers BLACT (beta-lactamase phenotype) and MRS (methicillin resistance) indicate a potential for increased pathogenicity of the strains, possibly associated with the exchange of genetic material between mutant bacteria (Urban-Chmiel et al. 2022). It is

Table 3 Resistance profile presented by human-derived isolates

Classes	Antibiotics	No. of resistant isolates	(%)	Resistance markers
Penicillin	Ampicillin	5	100	BLACT
Glycopeptide	Vancomycin	0	0	MRS
Lipopeptide	Daptomycin	0	0.00	MRSA
Macrolides	Erythromycin	4	90	STAMLS
Oxazolidinone	Linezolid	0	0	-
Penicillin	Oxacillin	4	90	-
Penicillin	Penicillin G	5	100	-
Macrocycles	Rifampicin	0	0	-

MRS Methicillin−Resistant *Staphylococcus, MRSA* Methicillin−Resistant *Staphylococcus aureus, STAMLS* MLSB Phenotype of *Staphylococcus spp,BLACTStaphylococcus* producing beta−lactamases

further suggested that the development of adaptive processes may be stimulated by indiscriminate exposure to antimicrobials and/or the administration of sublethal doses.

In addition, the presence of the constitutive resistance marker MLSB (resistance to macrolides, lincosamides, and streptogramin B) mediated by the MRSA gene was observed in four of the five isolates. This phenomenon is associated with modification of the target site and antimicrobial inactivation, and is considered a rare phenotype (Miklasinska-Majdanik 2021). Macrolide resistance was corroborated by antibiogram results (Table 3).

Regarding the antimicrobial activity of the compounds, when the inhibitory and bactericidal potential of CEE-OC against the isolates was analyzed, a wide variation of results was observed for both the MIC and MBC, with a high susceptibility observed in most isolates, except for 73,853 (*S. aureus*), C1, and C2 (*Staphylococcus* spp.), which exhibited bactericidal effects only at high concentrations, showing susceptibility only at the highest concentration of the extract (Table 4). The antimicrobial activity presented by the extract may be related to the high concentration of antioxidants and phenolic acids present in its composition (Kabra et al. 2019; El-Zahar et al. 2022). The presence and activity of phenolic compounds are among the main factors responsible for the disruption of the cell membrane, which may occur through binding to bacterial adhesins (Jafari-Sales et al., 2019).

Furthermore, given that most of the constituents in plant extracts are hydrophobic, they can more easily penetrate the cell wall of Gram-positive bacteria (Zarei et al. 2021). Another factor that may have contributed to the antibacterial effect is the specific presence of flavonoids in the composition of the plant extract used. Investigations by (Xue et al. 2019) showed the ability of the substance to inhibit staphyloxanthin production and consequently interfere with the virulence of methicillin-resistant *Staphylococcus aureus* (MRSA). In the present study, the interference of the extract in pigment production was not evaluated; however, it can be suggested that such interference may occur, since these compounds may block cellular signaling, as suggested by their antibacterial effect (Pachaiappan et al. 2022).

MIC results using AgNPs-OC ranged from 1:4 to 1:1, indicating a better degree of inhibition for the *S. capitis* (JCS) isolates with a ratio of 1:4, followed by *S. aureus* (AL01, AL02, WE08, WE09) and *Staphylococcus* sp. (C1), with ratios of 1:2 and 1:1 for the other isolates. For the MBC, a predominant bactericidal effect was observed at the

Table 4 Minimum inhibitory concentration and minimum bactericidal concentration of the crude ethanolic extract of *O. campechianum*, silver nanoparticles synthesized from crude ethanolic extract of *O. campechianum*, rosmarinic acid, non-commercial and commercial nanoparticles against *Staphylococcus* spp

	CEE-OC		AgNPs-OC		RA	AgNPs-NC	AgNPs-C
Isolates	MIC (µg/mL)	MBC (µg/mL)	MIC (µg/mL)	MBC (µg/mL)	MIC and MBC (µg/mL)	MIC and MBC (µg/mL)	MIC and MBC (µg/mL)
C1	6,250	12,500	1:2*	1:2*	NA	>1:1*	>10,000
C2	6,250	12,500	1:1*	1:1*	NA	>1:1*	>10,000
Q1	6,250	6,500	1:1*	1:1*	5,000	>1:1*	>10,000
Q2	6,250	6,250	1:1*	1:1*	NA	>1:1*	>10,000
Q3	6,250	6,250	1:1*	1:1*	NA	>1:1*	>10,000
IMA	6,250	6,250	1:1*	1:1*	NA	>1:1*	>10,000
EOC	781.25	781.25	1:1*	1:2*	1,250	>1:1*	>10,000
JCS	1,562	1,562	1:4*	1:2*	5,000	>1:1*	>10,000
RPS	3,125	3,125	1:1*	1:1*	NA	>1:1*	>10,000
HUT	6,250	6,250	1:1*	1:1*	5,000	>1:1*	>10,000
TH	3,125	3,125	1:1*	1:1*	NA	>1:1*	>10,000
ZO	3,125	3,125	1:1*	1:1*	NA	>1:1*	>10,000
AR	3,125	3,125	1:1*	1:1*	NA	>1:1*	>10,000
141/15	1,562	3,125	1:1*	1:1*	NA	>1:1*	>10,000
73853	1,562	12,500	1:1*	1:1*	NA	>1:1*	>10,000
FI	6,250	6,250	1:1*	1:1*	NA	>1:1*	>10,000
AL01	3,125	3,125	1:2*	1:2*	NA	>1:1*	>10,000
AL02	3,125	3,125	1:2*	1:2*	NA	>1:1*	>10,000
WE08	3,125	3,125	1:2*	1:2*	NA	>1:1*	>10,000
WE09	3,125	3,125	1:2*	1:2*	NA	>1:1*	>10,000
ATCC29213	3,125	3,125	1:2*	1:1*	5,000	>1:1*	>10,000

* Estimated concentration

NA not assessed, *MBC* Minimum bactericidal concentration, *MIC* Minimum inhibitory concentration, *CEE-OC* crude ethanolic extract of *O. campechianum*, *AgNPs-OC* silver nanoparticles synthesized from crude ethanolic extract of *O. campechianum*, *RA* rosmarinic acid, *AgNPs-NC* non-commercial nanoparticles, *AgNPs-C* commercial nanoparticles

highest estimated concentration (1:1). Although the results reported by (Singh et al. 2021) demonstrate that biosynthesis shows better activity when aqueous extracts are used, in the present study it was not possible to make a precise comparison due to the concentration of CEE-OC used for nanoparticle production, which differs from that used by the aforementioned authors. However, the antimicrobial effect of the extract may have been enhanced through biosynthesis, considering the fraction of the plant extract used for its production. However, the antimicrobial activity of the extract cannot be compared to that of the biosynthesized nanoparticles, since the initial concentration of CEE-OC for MIC evaluation was 12,500 µg/mL, and it was not possible to determine the initial concentration of AgNPs-OC, which was therefore only estimated.

Moreover, some factors may have contributed to the greater activity of AgNPs-OC, such as the relatively low colloidal stability observed (Zeta Potential = -29.5 mV), which may suggest a lower concentration of phenolic compounds (Cheung and Otto 2018; Lim et al. 2023). However, a relevant bactericidal effect was still observed, which, according to (Bouaquina et al. 2022), can be explained by the reactivity of the green-synthesized silver nanoparticles generated in the presence of these compounds with the proteins present in the bacterial cell wall, potentially interfering with bacterial genetic material replication.

In this study, the best results were observed for CEE-OC, which can be attributed to the fact that it was used in a higher concentration for the analyses. It is worth emphasizing that the antibacterial activity presented by the plant extract of wild sweet basil (CEE-OC) may be related to the chemotypes of the plant. According to (Bomma et al. 2020), some compounds present in plants can be influenced by the harvest season and soil type. Thus, it is possible to suggest that high-sunlight environments, such as the Caatinga Biome in the Brazilian Northeast where the plant was collected, may have contributed to its antimicrobial activity.

Additionally, a synergistic interaction may have occurred between the compounds present in the plant extract used for nanoparticle production, with the activity of major compounds potentially predominating such as rosmarinic acid, since it was the most abundant constituent identified in the extract. According to (Ivanov et al. 2022), phenolic compounds, such as rosmarinic acid, directly affect cell membrane permeability. It is likely that this compound stood out among the other constituents as a contributor to bacterial cell death.

The data also revealed both inhibitory and bactericidal activity at high concentrations, predominantly at 5 mg/mL of rosmarinic acid (RA) for the HUT, JCS, and Q1 isolates, as well as ATCC29213, except for the EOC isolate, which showed susceptibility at a concentration of 1,25 mg/mL (Table 4). The results obtained support the hypothesis that the antimicrobial effect of RA on *Staphylococcus* may be due to an interaction between the bioactive compound and the bacterial cell metabolism (Zhang et al. 2024). These findings corroborate those of (Iqbal et al. 2022), who showed significant antimicrobial activity of RA against antimicrobial-resistant Gram-positive bacteria, resulting in a reduction of more than 90% of the bacterial load in methicillin-resistant isolates. However, greater activity was observed when the plant extract was used, which suggests that RA may interact positively with the other constituents present in the extract. Similar results were observed by (Kernou et al. 2023), who reported enhanced activity when RA was combined with other antimicrobials, such as vancomycin, compared to their individual activities.

Regarding commercial and non-commercial (chemical synthesis) nanoparticles, no antibacterial activity was observed against *Staphylococcus* isolates (Table 4). The lack of activity observed is likely associated with the structural size of the nanoparticles, as the AgNPs-C used in this study were 20 nm in size, whereas greater antimicrobial activity has been reported for smaller particles (Aldayel et al. 2023). According to (Salomoni et al. 2017), nanoparticles smaller than 10 nm may provide greater availability of silver ions within bacterial cells. Based on this, this factor may have contributed, reducing the binding of silver to proteins present in the bacterial cell membrane and wall, thereby reducing its antimicrobial activity.

The analysis of the interaction between CEE-OC and AgNPs-OC (Table 5) showed more pronounced inhibitory activity when the compounds were combined than used individually, which was possibly enhanced by the higher concentration of plant-derived metabolites. The combination of these antimicrobial substances resulted in synergistic responses for 12 of the 20 isolates analyzed (60%), and additive responses for the others (25%). The results showed a reduction in MIC by up to 16x and 128x for CEE-OC and AgNPs-OC, respectively, although it is not possible to estimate the reduction in the concentration of each compound.

The synergistic effect observed may be due to the potentiation or facilitation of the binding of the different compounds analyzed, as reported by (Zarei et al. 2021. On the other hand, the observed additive effect may be attributed to the increased concentration resulting from the combination of the compounds, with their effects being additive. Therefore, the results observed for the isolates Q1, Q3, C2, AR, TH, 141/15, RPS, and ZO suggest a lack of synergistic or antagonistic interactions between the compounds. This outcome may be associated with the functional groups present in the bioactive components.

Table 5 Interaction between the crude ethanolic extract of *O. Campechianum* and the biosynthesized nanoparticles of *O. Campechianum*

Isolates	Tested substances	MIC (µg/mL)		∑FIC	Results
		Alone	Combined		
Q1	CEE-OC	6,250	390.62	1.250	Indifferent
	AgNPs-OC	1:1*	1:2*		
Q2	CEE-OC	6,250	1,562	0.281	Synergistic
	AgNPs-OC	1:1*	1:64*		
Q3	CEE-OC	6,250	781.25	1.125	Indifferent
	AgNPs-OC	1:1*	1:8*		
C1	CEE-OC	6,250	390.62	0.312	Synergistic
	AgNPs-OC	1:2*	1:8*		
C2	CEE-OC	6,250	3,125	0.553	Additive
	AgNPs-OC	1:1*	1:64*		
IMA	CEE-OC	6,250	1,562	0.281	Synergistic
	AgNPs-OC	1:1*	1:32*		
EOC	CEE-OC	782.25	98.00	0.375	Synergistic
	AgNPs-OC	1:1*	1:4*		
AL01	CEE-OC	3,125	390.62	0.156	Synergistic
	AgNPs-OC	1:2*	1:128*		
AR	CEE-OC	3,125	1,562	0.531	Additive
	AgNPs-OC	1:1*	1:64*		
HUT	CEE-OC	6,250	1,562	0.281	Synergistic
	AgNPs-OC	1:1*	1:64*		
JCS	CEE-OC	1,562	196.00	0.188	Synergistic
	AgNPs-OC	1:4*	1:64*		
FI	CEE-OC	6,250	1,562	0.499	Synergistic
	AgNPs-OC	1:1*	1:4*		
AL02	CEE-OC	3,125	781.25	0.281	Synergistic
	AgNPs-OC	1:2*	1:128*		
WE09	CEE-OC	3,125	390.62	0.156	Synergistic
	AgNPs-OC	1:2*	1:128*		
WE08	CEE-OC	3,125	390.62	0.156	Synergistic
	AgNPs-OC	1:2*	1:128*		
TH	CEE-OC	3,125	1,562	0.531	Additive
	AgNPs-OC	1:1*	1:64*		
141/15	CEE-OC	1,562	781.25	0.532	Additive
	AgNPs-OC	1:1*	1:64*		
RPS	CEE-OC	3,125	1,562	1.031	Indifferent
	AgNPs-OC	1:1*	1:64*		
ZO	CEE-OC	3,125	1,562	0.531	Additive
	AgNPs-OC	1:1*	1:64*		
73853	CEE-OC	1,532	781.25	0.156	Synergistic
	AgNPs-OC	1:2*	1:128*		

* Estimated concentration

∑*FIC* Fractional inhibitory concentration index, *CEE−OC* crude crude ethanolic extract of *O. Campechianum,AgNPs−OC* biosynthesized nanoparticles of *O. Campechianum*

According to (Bao et al. 2020) and (Antunes et al. 2023), the activity of silver nanoparticles can be increased when combined with other antimicrobial agents. A similar phenomenon has been observed with the combination of secondary metabolites, such as terpenoids and phenolic acids, which reinforces the hypothesis that the low concentration of bioactive compounds from CEE-OC used in nanoparticle synthesis may have reduced their efficacy in the broth microdilution assay.

Furthermore, it is suggested that, even at low concentrations, the antimicrobial inhibitory effect of the extract may still be evidenced when incorporated into the nanoparticles. Additionally, the enhanced activity observed with the increased concentration and the amount of the same active compound present in the extract suggests an interaction between antimicrobial agents in the medium, or the absence of such interactions in isolates that exhibited additive effects.

No synergistic interaction was observed between CEE-OC and AgNPs-C (Table 6). According to the analysis results, the substances may have interfered with each other's activity, possibly resulting in an antagonistic effect. It was also observed that increasing the concentration of CEE-OC did not alter the results, indicating a dose-independent effect. When analyzing the interaction between CEE-OC and AgNPs-NC (Table 6), a predominant antagonistic effect was observed among the isolates tested, with four of the six isolates classified as showing this type of interaction and the others classified as indifferent.

It is suggested that low stability and, particularly, the size of AgNPs-NC may have interfered with their antibacterial activity. According to (Cheon et al. 2019), unstable nanoparticles of varying sizes may release smaller amounts of silver ions, leading to the hypothesis that small amounts of nanoparticles may have entered the bacterial cells and released sublethal amounts of silver ions, with no significant interaction with Ca^{2+} within the bacterial cells.

Based on biofilm quantification, with ATCC29213 used as a strong biofilm producer control, it was observed that 25% of the 20 isolates showed strong biofilm production (WE08; WE09; HUT; AR; 141/15), 30% moderate (C2; Q3; FI; JCS; TH; ZO), 35% weak (AL01; AL02; C1; Q1; Q2; EOC; 73853), and 10% did not produce biofilms (IMA; RPS) (Fig. 4). Among 90% of isolates that produced biofilms, ten were of animal origin, five were from food, and three were of human origin.

These results indicate that biofilm production was present in isolates from all sources; including food, animal, and human sources. This mechanism is described by (Ballah et al. 2022) as a means of bacterial protection, survival, and adhesion to surfaces and different environments. The diversity of the environments from which the isolates in this study originated, along with favorable conditions for the development of this bacterial protection structure likely contributed to the high percentage of isolates exhibiting this characteristic.

However, a higher number of biofilm-producing isolates were of animal sources. Of these, four out of twenty isolates came from bovine mastitis, that is, from milk-producing animals intended for human consumption, followed by food sources such as cheese and meat, which accounted for five of the twenty isolates. Based on these results, we can infer that contaminated food may contribute to the spread of pathogenic bacteria.

Table 6 Interaction between the crude ethanolic extract of *O. Campechianum* and the commercial nanoparticles, and interaction between the crude ethanolic extract of *O. Campechianum* and the non-commercial nanoparticles

Isolates	Tested substances	MIC (µg/mL)		Results
		Alone	Combined	
HUT	CEE-OC	6,250	>6,250	Antagonistic
	AgNPs-C	>10,00	>10,00	
	CEE-OC	6,250	>6,250	
	AgNPs-NC	>1/1	>1/1	
JCS	CEE-OC	1,562	>1,562	Antagonistic
	AgNPs-C	>10,00	>10,00	
	CEE-OC	1,562	>1,562	
	AgNPs-NC	>1/1	>1/1	
EOC	CEE-OC	781.25	>781.25	Antagonistic
	AgNPs-C	>10,00	>10,00	
	CEE-OC	781.25	>781.25	
	AgNPs-NC	>1/1	>1/1	
IMA	CEE-OC	6,250	>6,250	Indifferent
	AgNPs-C	>10,00	>10,00	
	CEE-OC	6,250	6,250	
	AgNPs-NC	>1/1	>1/1	
RPS	CEE-OC	3,125	>3,125	Antagonistic
	AgNPs-C	>10,00	>10.00	
	CEE-OC	3,125	>3,125	
	AgNPs-NC	>1/1	>1/1	
ATCC29213	CEE-OC	3,125	>3,125	Antagonistic
	AgNPs-C	>10,00	>10,00	
	CEE-OC	3,125	>3,125	
	AgNPs-NC	>1/1	>1/1	

$\sum FIC$ Fractional inhibitory concentration index, *CEE−OC* crude crude ethanolic extract of *O. Campechianum*, *AgNPs−C* commercial nanoparticles, *AgNPs−CN* non commercial nanoparticles

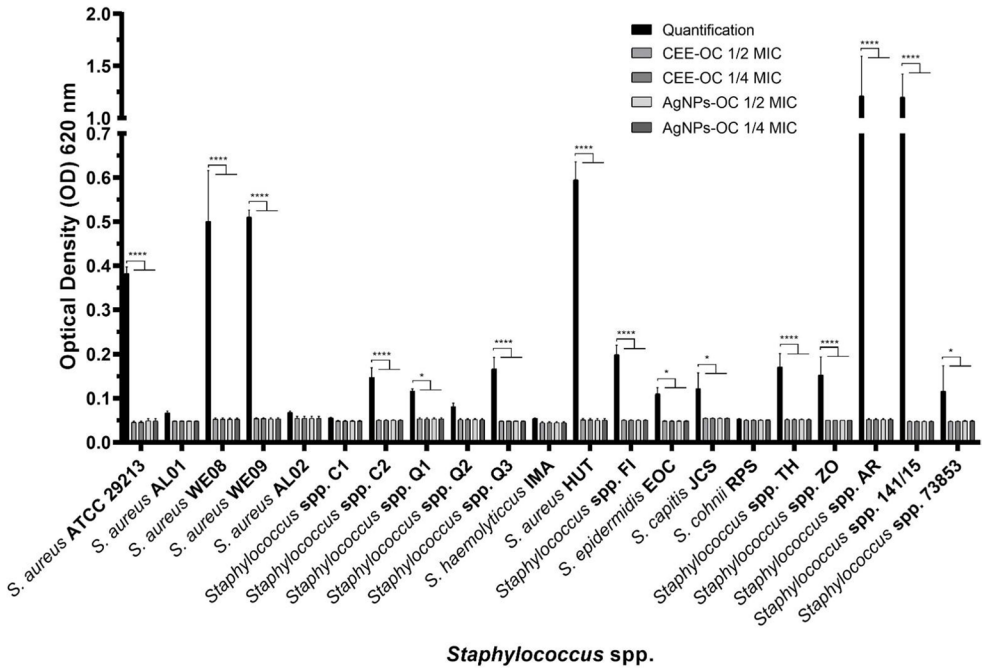

Fig. 4 Average optical densities comparison of quantification and interference of plant extract of *O. campechianum* (CEE-OC) and biogenic nanoparticles (AgNPs-OC) in biofilm formation by *Staphylococcus* spp

Regarding antibiofilm activity, both CEE-OC and AgNPs-OC significantly reduced biofilm formation in almost all isolates (WE08, WE09, C2, Q1, Q3, HUT, FI, EOC, JCS, TH, ZO, AR, 141/15, and 73853) and ATCC29213, with statistically significant differences observed at both inhibitory (½ CIM) and subinhibitory (¼ MIC) concentrations (Fig. 4). Isolates classified as strong, moderate and weak biofilm producers did not produce biofilm after the inclusion of the compounds mentioned above. Similar results were found by (Almatroudi et al. 2020) and (Fernandes et al. 2023), who observed interference in biofilm formation structure at low concentrations of silver nanoparticle biosynthesis. The results suggest that CEE-OC and AgNPs-OC mainly interfere with the early stages of biofilm development by affecting bacterial adhesion to the abiotic surface, consequently preventing subsequent colonization and biofilm formation.

Conversely, neither treatment showed activity against previously established biofilms, suggesting that mature biofilms may exhibit increased tolerance due to structural complexity and reduced antimicrobial penetration.

According to (Saeloh 2021), antimicrobials are less effective against biofilm-producing bacteria. However, although biofilm acts as a bacterial protective factor, it is not exclusively associated with a multiple drug resistance (MDR) profile. In this study, isolates classified as strong and moderate biofilm producers predominantly exhibited MDR. However, some isolates, such as AL02, Q1, and 73,853, which were classified as weak biofilm producers, were also identified as MDR, suggesting that, in addition to biofilm formation, other resistance-associated genes may be involved.

For AgNPs-NC, a significant reduction in biofilm formation (Fig. 5) was observed in *S. aureus* ATCC29213 and five clinical isolates (WE08, WE09, HUT, AR and, 141/15), all previously classified as strong biofilm producers, when exposed to a subinhibitory concentration at a 1:1 ratio. However, AgNPs-C did not exhibit inhibitory effects on biofilm formation in any of the analyzed isolates (Fig. 5).

In view of these results, it can be inferred that the slight reduction in biofilm production (from strong to moderate or weak) and/or temporary stabilization may be associated with the persistence and viability of non-planktonic cells and the lack of inhibition of the quorum sensing system, which is involved in biofilm formation and development (Abdelhamid and Yousef 2023). The other isolates showed no response to the activity of the substance. Similar to CEE-OC and AgNPs-OC, AgNPs-C and AgNPs-NC were also unable to interfere with established biofilms, as it was not possible to determine the MIC for these substances. In this case, it is suggested that the lack of interference with both biofilm formation and established biofilms may be related to the fact that the concentrations used — 10 µg/mL for AgNPs-C and 1:1 for AgNPs-NC — were insufficient to achieve inhibition, as concentrations at least fourfold higher would likely be required to effectively interfere with biofilm formation.

Molecular docking revealed a binding affinity of rosmarinic acid with six hydrogen bonds, three of which were formed with the polar amino acid ASN 340, and one each with ASN 137 (polar), GLU 222, and THR 223 (Fig. 6).

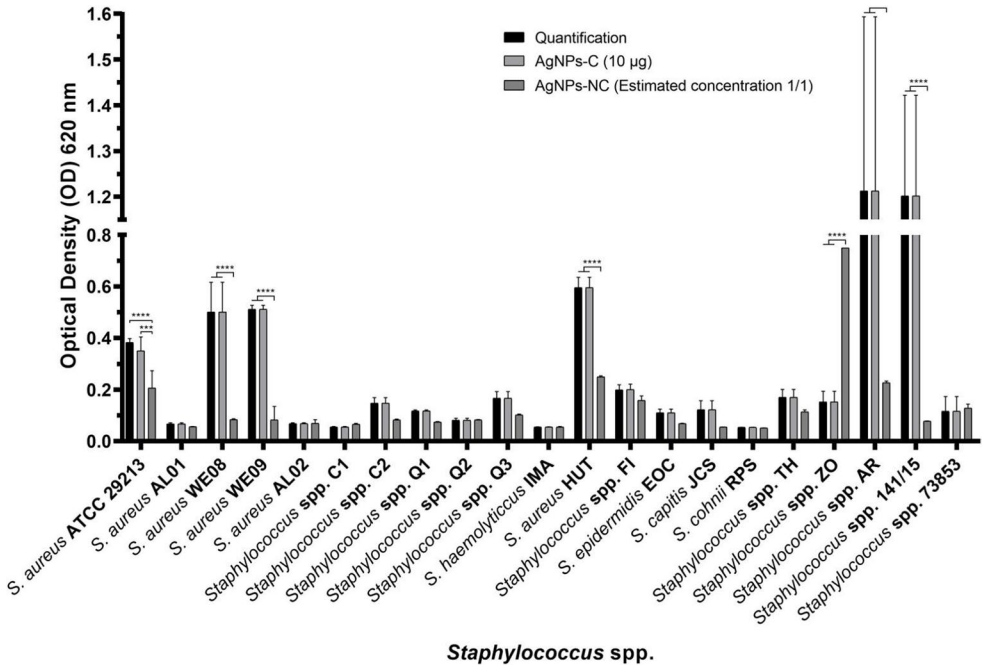

Fig. 5 Average optical densities comparison of quantification and interference of non-commercial (AgNPs-NC) and commercial (AgNPs-C) nanoparticles in biofilm formation by *Staphylococcus* spp

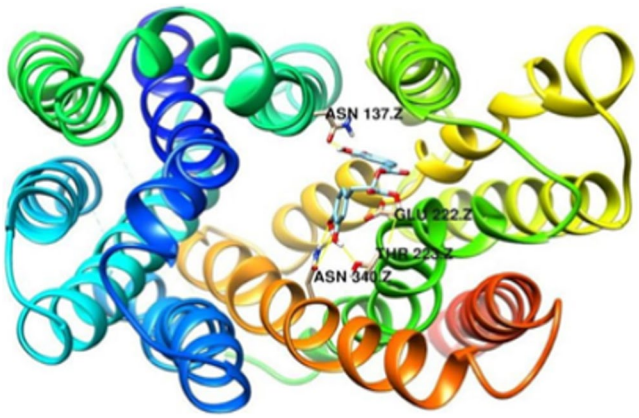

Fig. 6 Representation of the binding interactions between rosmarinic acid and the NorA protein of *S. aureus*

The in silico analysis indicated that rosmarinic acid may interact with NorA efflux pump protein through hydrogen bonds involving the ASN 340, GLU 222, ASN 137, and THR 223 residues. Thus, it is possible that staphylococci resistant to the quinolone class may become more susceptible, since interaction of rosmarinic acid with the NorA efflux pump could potentially interfere with this resistance mechanism involved in the efflux of these antimicrobials (Tintino et al. 2023). These results suggest that rosmarinic acid could potentially act as an adjuvant to quinolone antimicrobials. Regarding the bactericidal effects observed in the present study, it is suggested that this constituent may contribute to modulating resistance mechanisms in 25% of the isolates against this antimicrobial class, potentially resulting in increased susceptibility, particularly in the case of the plant extract, which contained higher concentrations of this compound.

Conclusion

The present study demonstrated the antimicrobial potential of the ethanolic extract of *O. campechianum* (CEE-OC) and silver nanoparticles biosynthesized from this extract (AgNPs-OC) against *Staphylococcus* spp., including multidrug-resistant strains. According to the molecular docking results, rosmarinic acid, identified as the major compound in the extract, showed potential interactions with the NorA efflux pump protein, which may contribute to the antimicrobial activity observed. Both substances also showed the ability to interfere with biofilm formation, although they had no effect on established biofilms. These findings highlight the potential relevance of these substances for preventive applications in clinical and healthcare settings. The absence of relevant antimicrobial activity by commercial (AgNPs-C) and non-commercial (AgNPs-NC) nanoparticles highlights the potential importance of plant-mediated biosynthesis in the functionalization of nanoparticles and enhancement of their antimicrobial activity. Thus, the results support the potential use of plant extracts and green nanotechnology as promising alternatives for addressing bacterial resistance. Future studies are needed to elucidate the mechanisms underlying these effects and to evaluate the in vivo efficacy of these substances.

Acknowledgements This study was financed in part by the Coordenação de Aperfeiçoamento de Pessoal de Nível Superior - Brasil (CAPES) - Finance Code 001, Conselho Nacional de Desenvolvimento Científico e Tecnológico (CNPq) – Process: 408695/2022-6; Fundação de Amparo à Ciência e Tecnologia do Estado de Pernambuco (FACEPE) - IBPG-1829-22-270723-0140, BFP-0150-5.05/22, APQ-1199-5.05/22, APQ-1895-5.05/24, APQ-2138-5.05/24).

Author contributions N.S.S. wrote the main manuscript text (writing original, validation, Project admnistration, investigation, data analyses). N.A. and M.M.C. (Supervision, Resources, Project administration, Funding acquisition, Conceptualization), A.K.J. (Formal analyses), M.L.G., J.P.S., T.M.S.S. and H.P.O. (Methodology and Formal analyses)

Funding The Article Processing Charge (APC) for the publication of this research was funded by the Coordenação de Aperfeiçoamento de Pessoal de Nível Superior - Brasil (CAPES) (ROR identifier: 00x0ma614). This study was financed in part by the Coordenação de Aperfeiçoamento de Pessoal de Nível Superior - Brasil (CAPES) - Finance Code 001, Conselho Nacional de Desenvolvimento Científico e Tecnológico (CNPq) – Process: 408695/2022-6; Fundação de Amparo à Ciência e Tecnologia do Estado de Pernambuco (FACEPE) - IBPG-1829-22-270723-0140, BFP-0150-5.05/22, APQ-1199-5.05/22, APQ-1895-5.05/24, APQ-2138-5.05/24).

Data availability The analyzed dataset on Dock Molecular in available in the Pubchem database. (https://pubchem.ncbi.nlm.nih.gov/compound/5281792). Other data are available upon request. Email natilene.vet@gmail.com.

Declarations

Ethics approval The research was approved by both CEUA (Comitê de Ética em Uso de Animais — Animal Use Ethics Committee) of the Federal University of the São Francisco Valley - UNIVASF, registered under No. 0002/300823, and CEP (Comitê de Ética em Pesquisa — Research Ethics Committee), registered under No. 6.013353. The isolates were identified under registration number AEEA0F9 and deposited in the Sistema Nacional de Gestão do Patrimônio Genético (National Genetic Heritage Management System). Furthermore, all human-derived bacterial isolates were anonymized and de-identified, with no access to patient information; therefore, informed consent was not required.

Consent to participate Not applicable.

Consent to publish Not applicable.

Competing interests The authors declare no competing interests.

References

Abdel-Aty AM, Barakat AZ, Bassuiny RI (2023) Statistical optimization, characterization, antioxidant and antibacterial properties of silver nanoparticle biosynthesized by saw palmetto seed phenolic extract. Sci Rep 13:115605. https://doi.org/10.1038/s41598-023-42675-0

Abdelhamid AG, Yousef AE (2023) Combating bacterial biofilms: Current and emerging antibiofilm strategies for treating persistent infections. Antibiotics 12:6: 1005. https://doi.org/10.3390/antibiotics12061005

Al-Audah S, Abdullah et al (2025) Biological effect of green synthesis of silver nanoparticles derived from Malva parviflora fruits. Int J Mol Sci 26:17: 8135. https://doi.org/10.3390/ijms26178135

Aldayel MF (2024) Biofabrication of silver nanoparticles using pergularia tomentosa extract and evaluation of their antibacterial, antioxidant, and cytotoxic properties. Life 14(12):1639. https://doi.org/10.3390/life14121639

Aldayel MF, El Semary N, Adams DG (2023) Differential antimicrobial effect of three-dimensional biogenic silver nanoparticles as broad-spectrum antibacterial agents against plant pathogens. Antibiotics 12(7):1114. https://doi.org/10.3390/antibiotics12071114

Alex AM, Subburaman S, Chauhan S, Ahuja V, Abdi G, Tarighat MA (2024) Green synthesis of silver nanoparticles prepared with Ocimum species and assessment of anticancer potential. Sci Rep 14:11707. https://doi.org/10.1038/s41598-024-61946-y

Almatroudi A, Khadri H, Azam M, Rahmani AH, Al Khaleefah FK, Khateef R, Ansari MA, Allemailem KS (2020) Antibacterial, antibiofilm and anticancer activity of biologically synthesized silver nanoparticles using seed extract of *Nigella sativa*. Processes 8:4388. https://doi.org/10.3390/pr8040388

Antunes Filho S, Dos Santos MS, Dos Santos AOL, Backx BP, Soran ML, Opriş O, Lung I, Stegarescu A, Bououdina M (2023) Biosynthesis of nanoparticles using plant extracts and essential oils. Molecules 28:73060. https://doi.org/10.3390/molecules28073060

Ashokkumar M, Palanisamy K, Kumar AG, Muthusamy C, Senthil Kumar KJ (2024) Green synthesis of silver and copper nanoparticles and their composites using Ocimum sanctum leaf extract displayed enhanced antibacterial, antioxidant and anticancer potentials. Artif Cells Nanomed Biotechnol 52(1):438–448. https://doi.org/10.1080/21691401.2024.2399938

Ballah FM, Islam MS, Rana ML, Ferdous FB, Ahmed R, Pramanik PK, Karmoker J, Ievy S, Sobur MA, Siddique MP, Khatun MM, Rahman M, Rahman MT (2022) Phenotypic and genotypic detection of biofilm-forming *Staphylococcus aureus* from different food sources in Bangladesh. Biology 11:7. https://doi.org/10.3390/biology11070949

Bao M, Zhang L, Liu B, Li L, Zhang Y, Zhao H, Ji X, Chen Q, Hu M, Bai J, Pang G, Yi J, Tan Y, Lu C (2020) Synergistic effects of anti-MRSA herbal extracts combined with antibiotics. Future Microbiol 151265–1276. https://doi.org/10.2217/fmb-2020-0001

Bomma M, Okafor F, Mentreddy SR, Nyochembeng L, Rangari VK, Khan S (2020) The chemical composition, characterization, and combination effect of *Ocimum campechianum* leaf essential oils and bio-produced silver nanoparticles against *Listeria monocytogenes* and *Escherichia coli*. Int J Curr Eng Technol 10:4: 518–526. https://doi.org/10.14741/ijcet/v.10.4.4

Bouaquina S, Aouf A, Touati A, Ali H, Elkhadragy M, Yehia H, Farouk A (2022) Effect of nanoencapsulation on the antimicrobial and antibiofilm activities of *algerian Origanum glandulosum* Desf. against multidrug- resistant clinical isolates. Nanomaterials 12:15: 2630. https://doi.org/10.3390/nano12152630

Bourbour S, Beigverdi R, Beheshti M, Jabalameli F, Emaneini M (2022) Identification of the main sequence types among strains of Staphylococcus aureus and *Staphylococcus*

epidermidis aminoglycoside-resistant strains isolated from clinical samples. Iran J Microbiol 14(3):305. https://doi.org/10.18502/ijm.v14i3.9760

Brawley DN, Sauer BD, Li J, Xuhui Z, Koide A, Jedhe G, Suwatthee T, Song J, Liu Z, Arora SP, Koide S, Torres JV, Wang DN, Traaseth N (2022) Structural basis for inhibition of the drug efflux pump NorA from *Staphylococcus aureus*. Nat Chem Biol 7(18):706–712. https://doi.org/10.1038/s41589-022-00994-9

Calvo-Irabien L (2025) María Essential Oil Variability of Ocimum campechianum Mill. in Southeastern Mexico: A Chemometric Approach. Chem Biodiv 22(12):E01898. https://doi.org/10.1002/cbdv.202501898

Cheon JY, Kim SJ, Rhee YH, Kwon OH, Park WH (2019) Shape-dependent antimicrobial activities of silver nanoparticles. Int J Nanomed 2773–2780. https://doi.org/10.2147/IJN.S196472

Cheung GYC, Otto M (2018) Do antimicrobial peptides and antimicrobial-peptide resistance play important roles during bacterial infection?. Future Microbiol 13:1073–1075. https://doi.org/10.2217/fmb-2018-0138

Chinnasamy R, Chinnaperumal K, Cherian T, Thamilchelvan K, Govindasamy B, Vetrivel C, Krutmuang P (2024) Eco-friendly phytofabrication of silver nanoparticles using aqueous extract of Aristolochia bracteolata Lam: its antioxidant potential, antibacterial activities against clinical pathogens and malarial larvicidal effects. Biomass Convers Biorefinery 14(22):28051–28066. https://doi.org/10.1007/s13399-023-03750-8

Clinical and Laboratory Standards Institute (CLSI) (2018) Methods for dilution antimicrobial susceptibility tests for bacteria that grow aerobically; approved standard. 11th ed. CLSI document M07. Wayne, PA: CLSI; pp 1-118

Cotter CJ, Ferradas C, Ludwig S, Dalton K, Larsen J, Laucks D, Davis MF (2023) Risk factors for meticillin-resistant *Staphylococcus aureus* (MRSA) carriage in MRSA-exposed household pets. Vet Dermatol 34(1):22–27. https://doi.org/10.1111/vde.13135

Eberhardt J, Santos-Martins D, Tillack AF, Forli (2021) AutoDock Vina 1.2. 0: new docking methods, expanded force field, and python bindings. J Chem Inf Model 618:3891–3898. https://doi.org/10.1021/acs.jcim.1c00203

El-Zahar KM, Al-Jamaan ME, Al-Mutairi FR, Al-Hudiab AM, Al-Einzi MS, Mohamed AAZ (2022) Antioxidant, antibacterial and antifungal activities of the ethanolic extract obtained from the roots and leaves of *Berberis vulgaris*. Molecules 27(18):6114. https://doi.org/10.3390/molecules27186114

Fatima S, Shahid H, Zafar S, Arooj I, Ijaz S, Elahi A (2024) Ocimum basilicum seed-mediated green synthesis of silver nanoparticles: characterization and evaluation of biological properties. Discov Nano 19:172. https://doi.org/10.1186/s11671-024-04130-5

Fernandes M, González-Ballesteros N, Da Costa A, Machado R, Gomes AC, Rodríguez-Argüelles MC (2023) Antimicrobial and anti-biofilm activity of silver nanoparticles biosynthesized with Cystoseira algae extracts. J Biol Inorg Chem 28(4):439–450. https://doi.org/10.1007/s00775-023-01999-y

Freire NB, Pires LC, Oliveira HP, Costa MM (2018) Antimicrobial and antibiofilm activity of silver nanoparticles on *Aeromonas spp*. isolates obtained from aquatic organisms. Brazilian Veterinary Res 38:244–249. https://doi.org/10.1590/1678-5150-PVB-4805

Guimarães ML, Da Silva FAG Jr, Da Costa MM, De Oliveira HP (2020) Green synthesis of silver nanoparticles using *Ziziphus* joazeiro leaf extract for production of antibacterial agents. Appl Nanosci 10:1073–1081. https://doi.org/10.1007/s13204-019-01181-4

Halanwani EM (2017) Rapid biosynthesis method and characterization of silver nanoparticles using *Zizyphus spina-christi* leaf extract and their antibacterial efficacy in therapeutic application. J Biomaterials Nanobiotechnol 8(1):22–35. https://doi.org/10.4236/jbnb.2017.81002

Huynh TQ, Tran VN, Thai VC, Nguyen HÁ, Nguyen NTG, Tran MK, Nguyen TTH (2023) Genomic alterations involved in the development of resistance to fluoroquinolones in *Staphylococcus aureus*. PLoS ONE 18:7. https://doi.org/10.1371/journal.pone.0287973

Iqbal H, Wright CL, Jones S, Da Silva GR, McKillen J, Gilmore BF, Green BD (2022) Extracts of Sida cordifolia contain polysaccharides possessing immunomodulatory activity and rosmarinic acid compounds with antibacterial activity. BMC Complement Med Ther 22:1: 27. https://doi.org/10.1186/s12906-022-03502-7

Ivanov M, Kostić M, Stojković D, Soković M (2022) Acid rosmarinic – Modes of antimicrobial and antibiofilm activities of a common plant polyphenol. J South Afr Bot 146:521–527. https://doi.org/10.1016/j.sajb.2021.11.050

Jafari-Sales A, Rasi-Bonab F, Sayyahi J (2019) The research on the antimicrobial effects of methanolic extract of *Carum copticum* L. on *Staphylococcus aureus*, *Bacillus cereus*, *Escherichia coli* and *Pseudomonas aeruginosa* under laboratory conditions. Military paramedic Health Science 13:4:19–25. https://doi.org/10.26655/jmchemsci.2020.2.2

Jiang JH, Cameron DR, Nethercott C, Aires-de-Sousa M, Peleg AY (2023) Virulence attributes of successful methicillin- resistant *Staphylococcus aureus* lineages. Clin Microbiol Rev 36:4:0014822. https://doi.org/10.1128/cmr.00148-22

Kabra A, Sharma R, Hano C, Kabra R, Martins N, Baghel US (2019) Phytochemical composition, antioxidant and antimicrobial attributes of different solvent extracts of Myrica esculenta Buch.-Ham. ex. D. Don Leaves. Biomolecules 9(8):357. https://doi.org/10.3390/biom9080357

Kang JY, Lee W, Noh GM, Jeong BH, Park I, Lee SJ (2020) Fluoroquinolone resistance of *Staphylococcus epidermidis* isolated from healthy conjunctiva and analysis of its mutations in the quinolone resistance determining region. Antimicrob Resist Infect Control 91–8. https://doi.org/10.1186/s13756-020-00841-3

Kernou O, Azzouz Z, Madani K, Rijo P (2023) Application of rosmarinic acid with its derivatives in the treatment of microbial pathogens. Molecules 28(10):4243. https://doi.org/10.3390/molecules28104243

Khosravi ADT, Jenabi A, Montazeri EA (2017) Distribution of genes encoding resistance to aminoglycoside-modifying enzymes in methicillin-resistant *Staphylococcus aureus* (MRSA) strains. Kaohsiung J Med Sci 33:12: 587–593. https://doi.org/10.1016/j.kjms.2017.08.001

Krumperman PH (1983) Multiple antibiotic resistance indexing of Escherichia coli to identify highrisk sources of fecal contamination of foods. Appl Environ Microbiol 46:1:165–170. https://doi.org/10.1128/aem.46.1.165-170.1983

Lim DY, Lee JS, Lee HG (2023) Nano-encapsulation of a combination of clove oil and thymol and their application in fresh-cut apples and raw minced beef. Food Control 148:109683. https://doi.org/10.1016/j.foodcont.2023.109683

Lee YS, Jang KA, Cha JD (2012) Synergistic antibacterial effect between silibinin and antibiotics in oral bacteria. J Biomed Biotechnol. https://doi.org/10.1155/2012/618081

Machado TS, Pinheiro FR, Andre LSP, Pereira RFA, Correa RF, De Mello GC, Aguiar-Alves F (2020) Virulence Factors Found in Nasal Colonization and Infection of Methicillin-Resistant *Staphylococcus aureus* (MRSA) Isolates and Their Ability to Form a Biofilm. Toxins (Basel) 13:1: 14. https://doi.org/10.3390/toxins13010014

Mandal K, Das D, Bose SK, Chaudhuri A, Chakraborty A, Mandal S, Ghosh S, Roy S (2024) Spectroscopic approach to optimize the biogenic silver nanoparticles for photocatalytic removal of ternary dye mixture and ecotoxicological impact of treated wastewater. Sci Rep 14:31174. https://doi.org/10.1038/s41598-024-82341-7

Manoharan M, Sistla S, Ray P (2021) Prevalence and Molecular Determinants of Antimicrobial Resistance in Clinical Isolates of *Staphylococcus haemolyticus* from India. Microb Drug Resist 27:4: 501–508. https://doi.org/10.1089/mdr.2019.0395

Merino N, Toledo-Arana A, Vergara-Irigaray M, Valle J, Solano C, Calvo E, Lasa I (2009) Protein A-Mediated Multicellular Behavior in *Staphylococcus aureus*. J Bacteriol 191:23: 832–843. https://doi.org/10.1128/jb.01222-08

Miklasinska-Majdanik M (2021) Mechanisms of resistance to macrolide antibiotics among *Staphylococcus aureus*. Antibiotics 10:11:1406. https://doi.org/10.3390/antibiotics10111406

Nostro A, Roccaro AS, Bisignano G, Marino A, Cannatelli MA, Pizzimenti FC, Blanco AR (2007) Effects of oregano, carvacrol and thymol on *Staphylococcus aureus* and *Staphylococcus epidermidis* biofilms. J Med Microbiol 56(4):519–523. https://doi.org/10.1099/jmm.0.46804-0

Pachaiappan R, Rajamuthu TP, Sarkar A, Natrajan P, Krishnan N, Sakthivelu M, Gopinath SC (2022) N-acyl-homoserine lactone mediated virulence factor (s) of *Pseudomonas aeruginosa* inhibited by flavonoids and isoflavonoids. Process Biochem 116:84–93. https://doi.org/10.1016/j.procbio.2022.02.024

Pugazhendhi A, Michael D, Prakash D, Krishnamaurthy PP, Shanmuganathan R, Al-Dhabi NA, Kaliannan T (2020) Antibiogram and plasmid profiling of beta-lactamase producing multi drug resistant *Staphylococcus aureus* isolated from poultry litter. J King Saud University-Science 32(6):2723–2727. https://doi.org/10.1016/j.jksus.2020.06.007

Rather MA, Gupta K, Mandal M (2021) Microbial biofilm: formation, architecture, antibiotic resistance, and control strategies. Brazilian J Microbiol 52(4):1701–1718. https://doi.org/10.1007/s42770-021-00624-x

Ruiz- Vargas JA, Morales-Ferra DL, Ramirez-Avila G, Zamilpa A, Negrete-Leon E, Acevedo-Fernández JJ, Pena-Rodriguez LM (2019) α-glicosidase inhibitory activity and in vivo antihyperglycemic effect of secondary metabolites from leaf infusion of *Ocimum campechianum mill*. J Ethnopharmacol 243112081. https://doi.org/10.1016/j.jep.2019.112081

Saeloh D, Visutthi M (2021) Efficacy of Thai plant extracts for antibacterial and anti- biofilm activities against pathogenic bacteria. Antibiotics 10:12: 1470. https://doi.org/10.3390/antibiotics10121470

Salomoni R, Léo P, Montemor AF, Rinaldi BG, Rodrigues MF (2017) Antibacterial effect of silver nanoparticles in *Pseudomonas aeruginosa*. Nanatechnol Sci Appl 115–121. https://doi.org/10.2147/NSA.S133415

Santos JP, Santos NS, Sant'ana AS, Silva JJ, Andreo N, Santos MWC, Costa MM (2025) Antimicrobial activity of plant extracts and compounds on resistant Gram-negative isolates from domestic animals. Brazilian Veterinary Res 45:e07570. https://doi.org/10.1590/1678-5150-PVB-7570

Scalvenzi L, Radice M, Toma L, Severini F, Boccolini D, Bella A, Di Luca M (2019) Larvicidal activity of Ocimum campechianum, Ocotea quixos and Piper aduncum essential oils against Aedes aegypti. Parasite. https://doi.org/10.1051/parasite/2019024

Schwarz S, Silley P, Simjee S, Woodford N, van Duijkeren E, Johnson AP, Gaastra W (2010) Assessing the antimicrobial susceptibility of bacteria obtained from animals. Vet Microbiol 141(1–2):1–4. https://doi.org/10.1093/jac/dkq037

Shah ST, Sari IP, Yanto DHY, Chowdhury ZZ, Bashir MN, Badruddin IA, Lee JS (2025) Nature' s nanofactories: Biogenic synthesis of metallic nanoparticles for sustainable technologies. Green Chem Lett Rev 18(1):2448171. https://doi.org/10.1080/17518253.2024.2448171

Siddiqi KS, Husen A, Rao RAK (2018) A review on biosynthesis of silver nanoparticles and their biocidal properties. J Nanobiotechnol 16:14. https://doi.org/10.1186/s12951-018-0334-5

Silva SEM, Costa M, Mendes RM, Morais C, Calhau MM (2016) Pintado, Antimicrobial, antiadhesive and antibiofilm activity of an ethanolic, anthocyanin-rich blueberry extract purified by solid phase extraction. J Appl Microbiol pg 693–703. https://doi.org/10.1111/jam.13215

Singh R, Hano C, Nath G, Sharma B (2021) Green Biosynthesis of Silver Nanoparticles Using Leaf Extract of Carissa carandas L. and Their Antioxidant and Antimicrobial Activity against Human Pathogenic Bacteria. Biomolecules 11:2: 299. https://doi.org/10.3390/biom11020299

Souza SA, Da Silva TMG, Da Silva SEM, Camara CA, Silva TMS (2018) Characterisation of phenolic compounds by UPLC-QTOF-MS/MS of geopropolis from the stingless bee *Melipona subnitida* (jandaíra). Phytochem Anal 29(6):549–558. https://doi.org/10.1002/pca.2766

Stepanovic S, Vuković D, Dakić I, Savić B, Švabić-Vlahović M (2000) A modified microtiter-plate test for quantification of staphylococcal biofilm formation. J Microbiol Methods 40:2: 175–179. https://doi.org/10.1016/S0167-7012(00)00122-6

Stepanovic S, Vukovic D, Hola V, Bonaventura G, Di, Djukic S, Cirkovic I, Ruzicka F (2007) Quantification of biofilm in microtiter plates: overview of testing conditions and practical recommendations for assessment of biofilm production by staphylococci. Apmis 115:891–899. https://doi.org/10.1111/j.1600-0463.2007

Szymanek-Majchrzak K, Mlynarczyk A, Kawecki D, Pacholczyk M, Durlik M, Deborska-Materkowska D, Mlynarczyk G (2018) Aminoglycoside resistance of methicillin- resistant *Staphylococcus aureus* strains originating from the surgical and transplant wards of the Warsaw clinical center- A retrospective analysis. In: Transplantation procedures. Elsevier 2170–2175. https://doi.org/10.1016/j.transproceed.2018.02.158

Tacchinni M, Echeverria Guevara MP, Grandini A, Maresca I, Radice M, Angiolella L, Guerrini A (2020) *Ocimum campechianum mill*. from Amazonian Ecuador: Chemical Composition and biological activities of extracts and their main constituents (eugenol and rosmarinic acid). Molecules 26:1: 84. https://doi.org/10.3390/molecules26010084

Tintino SR, Wilairatana P, De Souza VCA, Da Silva JMA, Pereira OS, De Morais Oliveira-Tintino CD, Balbino TCL (2023) Inhibition of the norA gene expression and the NorA efflux pump by the tannic acid. Sci Rep 13:1: 17394. https://doi.org/10.1038/s41598-023-43038-5

Urban-Chmiel R, Marek A, Stępień-Pyśniak D, Wieczorek K, Dec M, Nowaczek A, Osek J (2022) Antibiotic resistance in bacteria- a review. Antibiotics 11:81079. https://doi.org/10.3390/antibiotics11081079

Varghese RM, Kumar SA, Shanmugam R (2024) Antimicrobial Activity of Silver Nanoparticles Synthesized Using *Ocimum tenuiflorum* and *Ocimum gratissimum* Herbal Formulations. Cureus 26(2):e54994. https://doi.org/10.7759/cureus.54994

Wang N, Luo J, Deng F, Huang Y, Zhou H (2022) Combination antibiotic therapy: a strategy to overcome bacterial resistance to aminoglycoside antibiotics. Front Pharmacol 13839808. https://doi.org/10.3389/fphar.2022.839808

Xue L, Chen YY, Yan Z, Lu W, Wan D, Zhu H (2019) Staphyloxanthin: a potential target for antivirulence therapy. Infect drug Resist 2151–2160. https://doi.org/10.2147/IDR.S193649

Zarei YM, Ghazaei C, Maraghi ET, Bakhshi A, Shukohifar M (2021) Evaluation of antibacterial synergism of methanolic extract of *Dracocephalum kotschyi* e *Trachyspermum ammi*. Malays J Med Sci 28:6:64–75. https://doi.org/10.21315/mjms2021.28.6.7

Zhang J, Liu X, Zhang T, Bai B, Yang Y, Bo T, Fan S (2024) Study on the bacteriostatic property and bacteriostatic mechanism of the bacteriostatic agent composed of rosemarinic acid. Food bioscience 103820. https://doi.org/10.1016/j.fbio.2024.103820